Dalton Transactions

Cite this: *Dalton Trans.*, 2012, **41**, 14697

www.rsc.org/dalton

PAPER

The formation stability, hydrolytic behavior, mass spectrometry, DFT study, and luminescence properties of trivalent lanthanide complexes of H_2ODO2A†

C. Allen Chang,*[a,b,c] I-Fan Wang,[a] Hwa-Yu Lee,[b] Ching-Ning Meng,[b] Kuan-Yu Liu,[a,b] Ya-Fen Chen,[d,e] Tsai-Hua Yang,[b] Yun-Ming Wang[a] and Yeou-Guang Tsay[d,e]

Received 6th July 2012, Accepted 11th September 2012
DOI: 10.1039/c2dt31479g

The trivalent lanthanide complex formation constants (log K_f) of the macrocyclic ligand H_2ODO2A (4,10-dicarboxymethyl-1-oxa-4,7,10-triazacyclododecane) have been determined by pH titration techniques to be in the range 10.84–12.62 which increase with increasing lanthanide atomic number, and are smaller than those of the corresponding H_2DO2A (1,7-dicarboxylmethyl-1,4,7,10-tetraazacyclododecane) complexes. The equilibrium formation of the dinuclear hydrolysis species, *e.g.* $Ln_2(ODO2A)_2(\mu\text{-}OH)^+$ and $Ln_2(ODO2A)_2(\mu\text{-}OH)_2$, dominates over the mononuclear species, *e.g.* LnODO2A(OH) and $LnODO2A(OH)_2^-$. Mass spectrometry confirmed the presence of $[Eu(ODO2A)]^+$, $[Eu(ODO2A)(OH)+H]^+$, $[Eu_2(ODO2A)_2(OH)_2+H]^+$, $[Eu(ODO2A)(OH)_2]^-$ and $[Eu_2(ODO2A)_2(OH)_3]^-$ species at pH > 7. Density function theory (DFT) calculated structures of the $EuODO2A(H_2O)_3^+$ and $EuDO2A(H_2O)_3^+$ complexes indicate that three inner-sphere coordinated water molecules are arranged in a *meridional* configuration, *i.e.* the 3 water molecules are on the same plane perpendicular to that of the basal N_3O or N_4 atoms. However, luminescence lifetime studies reveal that the $EuODO2A^+$ and $TbODO2A^+$ complexes have 4.1 and 2.9 inner-sphere coordinated water molecules, respectively, indicating that other equilibrium species are also present for the $EuODO2A^+$ complex. The respective emission spectral intensities and lifetimes at 615 nm (λ_{ex} = 395 nm) and 544 nm (λ_{ex} = 369 nm) of the $EuODO2A^+$ and $TbODO2A^+$ complexes increase with increasing pH, consistent with the formation of μ-OH-bridged dinuclear species at higher pH. Additional DFT calculations show that each Y(III) ion is 8-coordinated in the three possible *cis*-$[Y_2(ODO2A)_2(\mu\text{-}OH)(H_2O)_2]^+$, *trans*-$[Y_2(ODO2A)_2(\mu\text{-}OH)\text{-}(H_2O)_2]^+$ and $[Y_2(ODO2A)_2(\mu\text{-}OH)_2]$ dinuclear complex structures. The first and the second include 6-coordination by the ligand $ODO2A^{2-}$, one by the bridged μ-OH ion and one by a water molecule. The third includes 6-coordination by the ligand $ODO2A^{2-}$ and two by the bridged μ-OH ions. The two inner-sphere coordinated water molecules in the *cis*- and *trans*-$[Y_2(ODO2A)_2(\mu\text{-}OH)(H_2O)_2]^+$ dinuclear complexes are in a staggered conformation with torsional angles of 82.21° and 148.54°, respectively.

Introduction

Trivalent lanthanide ions (Ln^{3+}) are hard Lewis acids and in aqueous solution they are usually 8–10 coordinated. When the Ln^{3+} ion, particularly Gd^{3+}, is coordinated with multidentate ligands that allow usually one inner-sphere coordinated water molecule, the resulting stable complexes have been used as effective magnetic resonance imaging (MRI) contrast agents, *e.g.* Magnevist, ProHance and Omniscan.[1] If the coordinated ligand or inner-sphere coordinated water molecules on the Ln^{3+} ion are able to be bio-activated (bio-responsive) or allow anion replacement, these systems could be used as molecular imaging agents[2] or luminescent anion sensors.[3] On the other hand, the coordinated water molecules could be hydrolyzed at relatively lower pH which makes them potentially good candidates as artificial nucleases, peptidases and hydrolases.[4]

Early research works on the hydrolysis of trivalent lanthanide ions are summarized in an excellent monograph.[5] Although a number of ligand-controlled self-assembly of polynuclear lanthanide-oxo/hydroxo complexes have been recently synthesized and characterized by crystallography,[6] except for the first hydrolysis constants leading to the formation of the mononuclear $Ln\text{-}OH^{2+}$ species,[7] the equilibrium constants for the formation of

[a]*Department of Biological Science and Technology, National Chiao Tung University, No. 75 Po-Ai Street, Hsinchu, Taiwan 30039, R. O. C.*
[b]*Department of Biomedical Imaging and Radiological Sciences, National Yang-Ming University, No. 155, Sec. 2, Li-Nong St., Beitou, Taipei, Taiwan 112, R. O. C. E-mail: cachang@ym.edu.tw; Fax: +886-2-28201093; Tel: +886-2-28201091*
[c]*Biophotonics & Molecular Imaging Research Center (BMIRC), National Yang-Ming University, Taipei, Taiwan, R. O. C.*
[d]*Proteomics Research Center, National Yang-Ming University, Taipei, Taiwan, R. O. C.*
[e]*Institute of Biochemistry & Molecular Biology, National Yang-Ming University, Taipei, Taiwan, R. O. C.*
†Electronic supplementary information (ESI) available. See DOI: 10.1039/c2dt31479g

polynuclear species such as $Ln_2(OH)_2^{4+}$, $Ln_3(OH)_5^{4+}$ and $Ln_5(OH)_9^{6+}$ could only be determined in high ionic strength media with limited accuracy, due to the complexity of various hydrolysis equilibria at high pH and easy hydroxide precipitation.

Formation of trivalent lanthanide complexes with multidentate ligands tends to reduce the number of the inner-coordinated water molecules and allow possibly better control of their hydrolysis behaviors. For example, the anionic $EuEDTA^-$ ($EDTA^{4-}$ = ethylenediamine-*N*,*N*,*N*′,*N*′-tetraacetate ion) and neutral EuHEDTA ($HEDTA^{3-}$ = *N*-hydroxylethyl(ethylenediamine)-*N*,*N*′,*N*′-triacetate ion) complexes have the respective coordinated water hydrolysis constants of pK_h = 12.48[8a] and pK_h = 10.1.[8b] However, for applications as artificial nucleases, recent studies suggested the use of stable and positively charged dinuclear lanthanide complexes with at least two or more inner-sphere coordinated water molecules.[9] In our laboratory, we have found that the $EuDO2A^+$ complex with 3 inner-sphere coordinated water molecules was able to promote phosphodiester bond hydrolysis with appreciable rates at pH 9–10 ($DO2A^{2-}$ is the deprotonated form of H_2DO2A, *i.e.* 1,7-dicarboxylmethyl-1,4,7,10-tetraazacyclododecane, Scheme 1).[10] It was proposed that the mono-hydroxo-bridged $Eu_2(DO2A)_2(\mu\text{-}OH)(OH)(H_2O)_3$ and the di-hydroxo-bridged $Eu_2(DO2A)_2(\mu\text{-}OH)_2(H_2O)_2$ species were more reactive than the mononuclear species. However, due to the slow complex formation rates, the formation constants for these μ-OH bridged dinuclear species could not be determined directly and accurately to further confirm exactly which species was the more reactive.[11]

Previously, we have found that the Ln(III) complex formation constants[12] of a number of oxaaza-macrocyclic diacetic acid ligands, *i.e.* H_2K21DA (dapda, 1,7-diaza-4,10,13-trioxacyclopentadecane-*N*,*N*′-diacetic acid,[12b] Scheme 1) and H_2K22DA (dacda, 1,10-diaza-4,7,13,16-tetraoxacyclooctadecane-*N*,*N*′-diacetic acid,[12a] Scheme 1) could be conveniently determined by pH titration techniques. In order to understand the formation stability, hydrolysis behaviors, and structures of trivalent lanthanide complexes better, we have synthesized the oxaaza-macrocyclic ligand, 4,10-dicarboxymethyl-1-oxa-4,7,10-triazacyclododecane (H_2ODO2A, Scheme 1),[13] and have determined their trivalent lanthanide complex stability constants and various formation constants involving hydroxide species. We have also studied mass spectrometry, solution luminescence properties[14] and density function theoretical (DFT) predictions of their structures.[15] The results are reported in this paper.

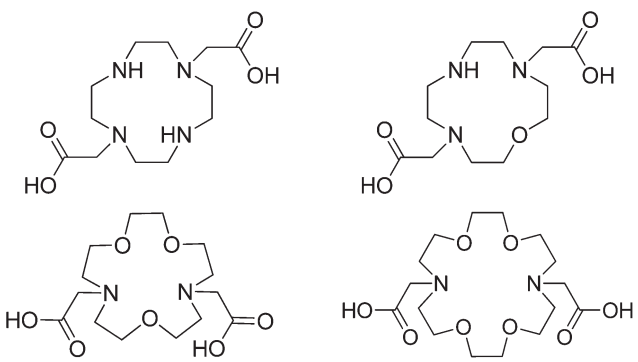

Scheme 1 Structural formulas of H_2DO2A (upper-left), H_2ODO2A (upper-right), H_2K21DA (lower-left) and H_2K22DA (lower-right).

Results and discussion

Synthesis and purification of H_2ODO2A

The synthesis of the ligand H_2ODO2A has been reported previously and is rather straightforward.[13] Protection of the middle secondary ring nitrogen atom from carboxymethylation can be done by controlling reaction solution pH because protonation of this more basic nitrogen atom occurs at high pH, *i.e.* the logarithmic first protonation constant of 1-oxa-4,7,10-triazacyclododecane is 10.11.[16a] Although the previously reported synthesis for the carboxymethylation reaction was performed at pH 8.5, in our hands we found that by keeping the pH to *ca.* 8.0 and using two equivalents of bromoacetate, the tris-carboxy-methylation by-product could be greatly reduced. This final purification of H_2ODO2A was performed by first passing the last reaction product solution through an anion exchange column, concentrating it, and then recrystallizing it in ethanolic HCl solution.

Ligand protonation constants and protonation sites of H_2ODO2A

The logarithmic protonation constants of H_2ODO2A determined by the potentiometric method are 11.08 ± 0.02, 5.96 ± 0.04, 2.85 ± 0.10, and 1.94 ± 0.10. These values are a little lower than those reported previously,[13] *i.e.* 11.24, 6.02, 2.94. The previously reported NMR titration experiments at various pH solutions were also repeated by us and similar results were obtained (Fig. S1, ESI†). The data concerning the protonation sequence were best explained by first protonation at the secondary ring nitrogen and second protonation on the tertiary ring nitrogen atoms with simultaneous partial deprotonation of the secondary ring nitrogen atom.

Stabilities of $LnODO2A^+$ complexes

Fluorescence titration by the molar ratio method indicated that Eu^{3+} and $ODO2A^{2-}$ at pH 6.7 form a 1 : 1 complex (λ_{ex} = 395 nm, λ_{em} = 615 nm; data not shown). Unlike those of $DO2A^{2-}$ complexes,[11] the kinetics are relatively faster for the formation reactions between the trivalent lanthanide ions and the ligand $ODO2A^{2-}$ due to faster equilibrium pH establishment after each addition of standard base, and the stability constants could be conveniently determined by potentiometric pH titration techniques. The logarithmic formation constants of the $LnODO2A^+$ complexes (including $YODO2A^+$) and their hydrolysis species (*vide infra*) are listed in Table 1. Scheme S1† shows the definitions of formation reactions and constants for these hydrolysis species (ESI,† L = ODO2A). For comparison purposes, the stability data of Ln^{3+} complexes of three structural analogues of $ODO2A^{2-}$, *i.e.* $DO2A^{2-}$, $K21DA^{2-}$ and $K22DA^{2-}$ are listed in Table S1 (ESI†) and plotted in Fig. 1. Fig. S2 (ESI†) shows some selected pH titration curves of $LnODO2A^+$.

The formation constants of the $LnODO2A^+$ complexes are in the range log K_f 10.84–12.62 and increase with increasing

Table 1 Formation constants of the Ln(III)-ODO2A^{2-} complex systems, 25 °C, ionic strength 0.1[a,b]

Ln	log β_{110}(log K_f)	log β_{111}	log $\beta_{22\text{-}1}$	log $\beta_{22\text{-}2}$	log $\beta_{22\text{-}3}$	log $\beta_{22\text{-}4}$
La	10.84 (0.02)	14.46 (0.41)	17.12 (0.09)	8.58 (0.10)	−0.10 (0.12)	−10.11 (0.08)
Ce	11.30 (0.01)	15.28 (0.06)	18.10 (0.08)	9.49 (0.08)	0.35 (0.08)	−9.52 (0.08)
Pr	11.98 (0.01)	15.28 (0.10)	19.66 (0.09)	11.21 (0.09)	0.82 (0.19)	−8.79 (0.09)
Nd	11.95 (0.01)	15.02 (0.22)	19.67 (0.08)	10.95 (0.11)	1.04 (0.11)	−8.94 (0.10)
Sm	12.41 (0.01)	16.01 (0.06)	20.50 (0.12)	12.38 (0.06)	1.90 (0.16)	−8.37 (0.10)
Eu	12.27 (0.01)	15.55 (0.13)	20.15 (0.17)	10.84 (0.25)	1.67 (0.16)	−9.15 (0.21)
Gd	12.00 (0.01)	—	19.38 (0.14)	9.88 (0.17)	−1.55 (0.58)	−11.97 (0.22)
Tb	12.13 (0.01)	—	19.87 (0.15)	12.06 (0.11)	2.23 (0.17)	−7.78 (0.12)
Dy	12.04 (0.01)	—	19.66 (0.14)	10.66 (0.16)	0.36 (0.18)	−10.85 (0.34)
Ho	12.04 (0.01)		19.82 (0.08)	11.66 (0.07)	1.55 (0.11)	−8.82 (0.09)
Er	12.04 (0.01)	—	19.93 (0.18)	11.76 (0.20)	2.03 (0.28)	−8.09 (0.25)
Tm	12.17 (0.01)	—	19.94 (0.22)	11.13 (0.25)	1.05 (0.27)	−9.59 (0.31)
Yb	12.62 (0.01)	—	20.90 (0.15)	13.23 (0.10)	4.05 (0.12)	−6.00 (0.12)
Lu	12.60 (0.01)	—	20.87 (0.12)	12.01 (0.24)	2.28 (0.25)	−7.49 (0.19)
Y	11.72 (0.02)		19.95 (0.20)	11.63 (0.18)	2.95 (0.18)	−7.59 (0.19)

[a] The overall protonation constants for ODO2A^{2-} are: log β_1, 11.08; log β_2, 17.04; log β_3, 19.89; log β_4, 21.83. [b] The formation constants were the averaged values of three to five determinations. Values in parentheses are the standard deviations of each formation constant. The averaged standard deviation values are as follows: log K_f, 0.01; log β_{111}, 0.16; log $\beta_{22\text{-}1}$, 0.13; log $\beta_{22\text{-}2}$, 0.14; log $\beta_{22\text{-}3}$, 0.20; log $\beta_{22\text{-}4}$, 0.17. The relatively larger standard deviation values for the species involving hydroxide formation (*i.e.* $Ln_2L_2H_{-3}$ and $Ln_2L_2H_{-4}$) are due to slower equilibria as compared to those of LnL.

lanthanide atomic number, to a greater extent for the lighter Ln(III) ions (*i.e.* La–Eu) and a lesser extent for the heavier Ln(III) ions (*i.e.* Gd–Lu). This indicates that electrostatic interaction is dominant between Ln^{3+} and ODO2A^{2-}. The phenomenon of gadolinium break seems also apparent. The LnODO2A$^+$ stability is usually smaller (*i.e.* up to 1.27log K units) than that of the corresponding LnDO2A$^+$. Thus, substituting one secondary nitrogen donor atom of the cyclen macrocycle of DO2A^{2-} by an ether donor atom to result in the ligand ODO2A^{2-} decreases the overall Ln^{3+} formation stability. At least three reasons are apparent. The first is that the basicity of ODO2A^{2-} as represented by the summation of the first three protonation constants (Σlog K = 19.89) is less than that of DO2A^{2-} (Σlog K = 24.34). Second, the rigidity of the macrocycle of ODO2A^{2-} is relatively less than that of DO2A^{2-} as manifested by the relatively faster LnODO2A$^+$ formation and dissociation kinetics (to be reported elsewhere). Third, the LnODO2A$^+$ complex is less symmetrical than the corresponding LnDO2A$^+$ and is more distorted and results in lower stabilization energy.

For macrocyclic ligands with ionizable coordinating pendant functional groups, the electrostatic interactions between the Ln(III) ions and the ligand are expected to increase as the charge density of the Ln(III) ion increases across the series due to lanthanide contraction. On the other hand, the match between the size of the macrocyclic cavity and the Ln(III) ion could tune the complex formation selectivity. A more careful examination of the stability trend of the lighter Ln(III)-ODO2A^{2-} complexes (*i.e.* La–Eu) indicates that it is similar to those of LnDO2A$^+$ and LnK21DA$^+$, as well as other macrocyclic aminopolycarboxylate complexes of DOTA^{4-} (1,4,7,10-tetra-azacyclododecane-1,4,7,10-tetraacetate ion), TETA^{4-} (1,4,8,11-tetraazacyclotetradecane-1,4,8,11-tetraacetate ion), PEPA^{5-} (1,4,7,10,13-pentaazacyclo-pentadecane-*N*,*N*′,*N*″,*N*‴,*N*⁗-pentaacetate ion) and HEHA^{6-} (1,4,7,10,13,16-hexaaza-cyclooctadecane-*N*,*N*′,*N*″,N‴,*N*⁗,*N*⁗′-hexaacetate ion),[17] consistent with the notion that electrostatic interaction dominates the lighter Ln(III)-cyclen macrocyclic

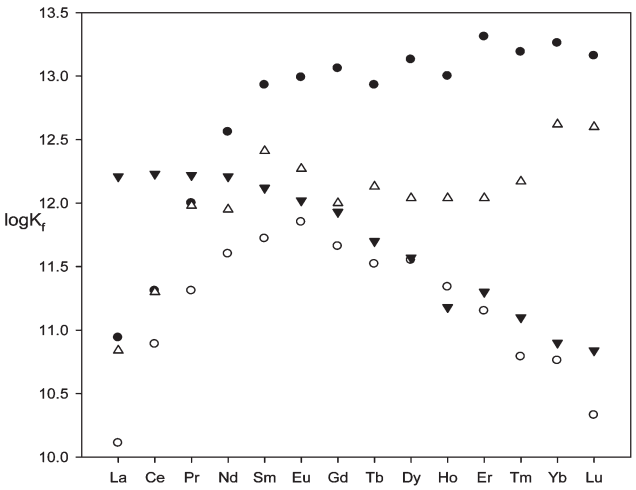

Fig. 1 Plots of the log K_f values for the Ln(III) complexes of ODO2A^{2-} (△), DO2A^{2-} (●), K21DA^{2-} (○) and K22DA^{2-} (▼). Data are from Table S1.†

complex formation. The ODO2A^{2-} macrocycle is too small to exert a size effect towards the lighter and larger Ln(III) ions. However, for the heavier Ln(III)-ODO2A^{2-} complexes (*i.e.* Gd–Lu), the observed trend suggests factors such as better fit between metal ion radius and ligand cavity size may be important. As the number of the ether oxygen atoms is increased and the macrocycle ring becomes larger, the flexibility of the macrocycle ring is increased and so are the modulations of the size effect to Ln(III) ion selectivities. This probably could be shown by the Δlog $K_{f,range}$ (*i.e.* log $K_{f,highest}$ − log $K_{f,lowerest}$) values. Among the ligands illustrated in this paper, the Δlog $K_{f,range}$ values are greater for lanthanide complexes with dominant ionic interactions (*e.g.* the respective Δlog $K_{f,range}$ values for DO2A^{2-}, TETA^{4-}, PEPA^{5-}, and HEHA^{6-} are 2.37, 2.57, 3.14 and 5.16 with selectivities towards the heavier lanthanides) and smaller

for those with more cavity size modulations (*e.g.* the respective $\Delta\log K_{f,range}$ values for $ODO2A^{2-}$, $K21DA^{2-}$ and $K22DA^{2-}$ are 1.78, 1.74, and 1.39 with selectivities varied from that for heavier, middle and lighter lanthanides, respectively). Note that an unprecedented selectivity for lighter lanthanides has been reported for a new macrocyclic ligand, *N*,*N*′-bis[(6-carboxy-2-pyridyl)methyl]-4,13-diaza-18-crown-6 with a $\Delta\log K_{f,range}$ of 6.86.[18] For analogous cationic complexes of $LnODO2A^{+}$, the stability trend is roughly $LnK22DA^{+} > LnDO2A^{+} \geq LnODO2A^{+} > LnK21DA^{+}$ for the lighter La–Eu complexes, with a few exceptions of the $LnK22DA^{+}$ and $LnDO2A^{+}$ complexes (*i.e.* Ln = Nd and Eu). For the heavier Gd–Lu complexes, the trend is roughly $LnDO2A^{+} > LnODO2A^{+} > LnK22DA^{+} > LnK21DA^{+}$ presumably due to the larger ring size flexibilities of the K21DA/K22DA ligands and the interplay of the overall greater basicity and ring rigidity of the DO2A/ODO2A ligands.

The protonation constants of the lanthanide complexes (log *K*′) could be obtained by the differences between the corresponding log β_{111} and log K_f(log β_{110}) values. Our titration data allow the calculations of these values only for six lighter $LnODO2A^{+}$ (Ln = La–Eu) complexes and they are in the range 3.28–3.98. These values are similar to those of the $LnDO2A^{+}$ complex, *i.e.* 3.20–3.98[19a] and the $LnK21DA^{+}$ complex, *i.e.* 3.47–4.24[19b] determined from kinetic studies. These values are consistent with the proposition that protonation is on the carboxylate functional groups of these complexes.

Hydrolytic behaviors of the $LnODO2A^{+}$ complexes in aqueous solution

It is also noted that the titration curves became much more complex after roughly 5 equivalents of base were added (Fig. S2, ESI†). Fitting these data to the equilibrium and hydrolysis model shown in Fig. 2 leads to much more interesting and significant results involving μ-OH bridged dinuclear $Ln_2L_2(\mu\text{-}OH)_n$ (n = 1–2) species formation with smaller deviations. Note that when mononuclear hydroxide species were included, the data fittings in most cases either wouldn't converge or converged with larger deviations. To our knowledge, although seemingly straightforward, this general behavior has not been reported previously in a complete and systematic fashion. It is also noted that this scheme was not reported when transition metal (*e.g.* Cu(II) and Zn(II)) oxatriaza complexes were studied because those complexes preferred simple stepwise mononuclear hydroxide species formation.[16]

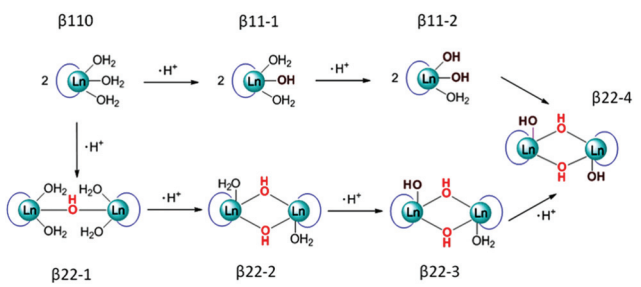

Fig. 2 A proposed general hydrolysis scheme for some of trivalent lanthanide $ODO2A^{2-}$ complexes.

Depending on the ionic radius of the Ln^{3+} ion, the number of inner-sphere coordinated water molecules could be 2, 3, or 4 if the 6-coordinating $ODO2A^{2-}$ is already coordinated to the Ln^{3+} ion. For a smaller Ln(III) ion (*e.g.* Yb^{3+} and Lu^{3+}) and for the macrocyclic ligands which result in the formation of Ln(III) complexes with two inner-sphere coordinated water molecules (*e.g.* $DO2A^{2-}$, $ODO2A^{2-}$ and Ln-$K21DA^{2-}$,[14]), the number of major dinuclear μ-OH bridged species would be two, *i.e.* $Ln_2L_2(\mu\text{-}OH)$ and $Ln_2L_2(\mu\text{-}OH)_2$. More careful examinations of the speciation diagrams (*e.g.* Fig. 3) reveal that: (1) the μ-OH bridged $Ln_2L_2(\mu\text{-}OH)$ species is always formed before LnL(OH); (2) $Ln_2L_2(\mu\text{-}OH)$ is formed prior to $Ln_2L_2(\mu\text{-}OH)_2$, $Ln_2L_2(\mu\text{-}OH)_2(OH)^{-}$, and $Ln_2L_2(\mu\text{-}OH)_2(OH)_2^{2-}$, and its stability gradually increases slightly with increasing atomic number, however, the relative species abundances are not always easily predicable; (3) the equilibrium formation of the mononuclear species (*e.g.* LnL(OH) and $LnL(OH)_2^{-}$) is less significant as compared to the dinuclear species; (4) the log $\beta_{22\text{-}3}$ and log $\beta_{22\text{-}4}$ values are subjected to larger uncertainties due to relatively larger measured errors at higher pH, and systematic trends are not obviously observed.

Fig. 3 shows the speciation diagrams of the La(III)-$ODO2A^{2-}$, Eu(III)-$ODO2A^{2-}$ and Yb(III)-$ODO2A^{2-}$ complex systems. It is observed that although maximum $EuODO2A^{+}$ formation occurs at a lower pH (*i.e.* pH 5.5) than that of $LaODO2A^{+}$ (pH ~ 6.0), the maximum formations of the μ-OH bridged dinuclear $La_2L_2(\mu\text{-}OH)_n(OH)_m$ (m,n = 1,2) species all occur at lower pH than the corresponding $Eu_2L_2(\mu\text{-}OH)_n(OH)_m$ (m,n = 1,2) species. On the other hand, 95% of $YbODO2A^{+}$ forms at pH 5.4 which is lower than those of $LaODO2A^{+}$ and $EuODO2A^{+}$, the maximum formations of the μ-OH bridged dinuclear $Yb_2L_2(\mu\text{-}OH)_n(OH)_m$ (m,n = 1,2) species both occur at lower pH than the corresponding $La_2L_2(\mu\text{-}OH)_n(OH)_m$ (m, n = 1,2) species. Similar data have also been found for other macrocyclic ligand systems such as H_2NO2A (4,7-dicarboxymethyl-1,4,7-triazacyclononane) and H_2ONO2A (4,7-dicarboxymethyl-1-oxa-4,7-diazacyclononane) but could not be obtained with traditional linear ligands such as ethylenediamine-*N*,*N*′-diacetic acid (H_2EDDA) nor those with easy hydroxide precipitation. These results will be reported elsewhere.

Mass spectrometry

Both the positive and negative ESI-MS spectral data of the Eu(III)-$ODO2A^{2-}$ complex system confirmed the presence of the hydrolytic, mono- and di-nuclear species. The ESI-MS(+) peaks for the $[Eu(ODO2A)]^{+}$ species (m/z at 438, 440), $[Eu(ODO2A)(OH) + H]^{+}$ species (m/z at 456 and 458) and for the $[Eu_2(ODO2A)_2(OH_2)_2 + H]^{+}$ species (m/z at 911, 913 and 915) could be observed at pH 7.36 (Fig. 4). The ESI-MS(−) peaks for the $[Eu(ODO2A)(OH)_2]^{-}$ species (m/z at 472 and 474) and for the $[Eu_2(ODO2A)_2(OH_2)_3]^{-}$ species (m/z at 927, 929 and 931) could be observed at pH 8.28 (Fig. S3, ESI†). It is noteworthy that, due to the distinct ionization energies of the mononuclear and dinuclear species, it is very likely that these ions in solution could not be quantitatively compared according to their signals in mass spectrometry.

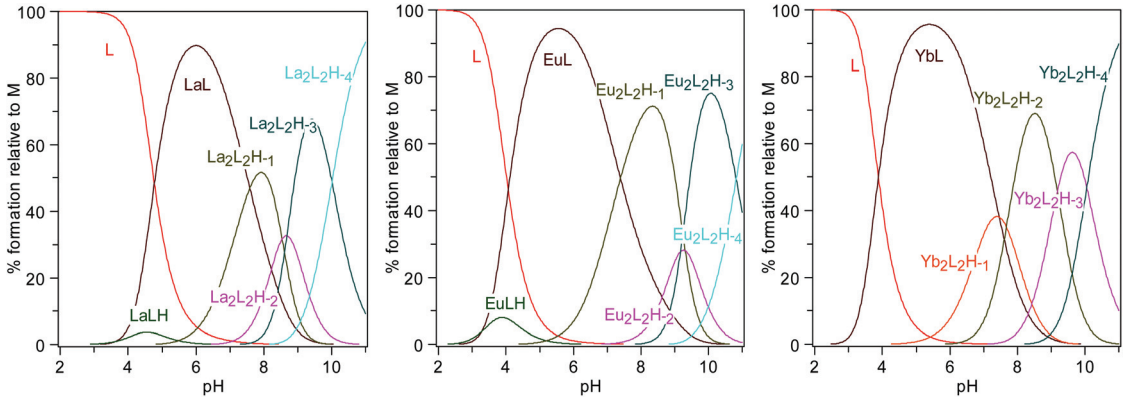

Fig. 3 Speciation diagrams of the La(III)-ODO2A^{2-} (left), Eu(III)-ODO2A^{2-} (middle) and Yb(III)-ODO2A^{2-} (right) complex systems. [La(III)] = [Eu(III)] = [Yb(III)] = [ODO2A^{2-}(L^{2-})] = 0.001 M.

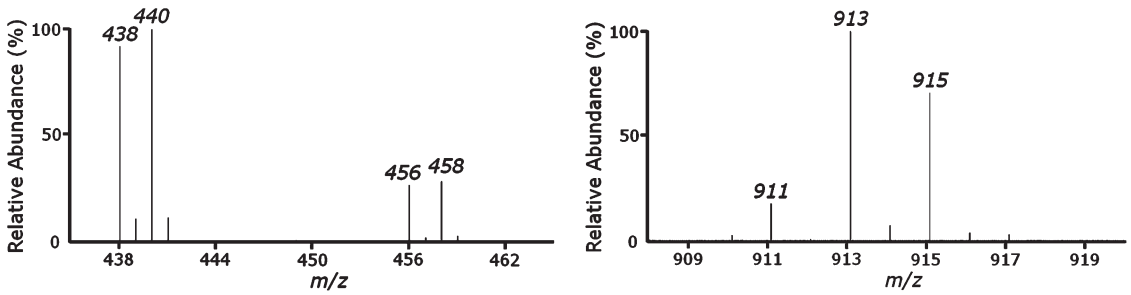

Fig. 4 ESI-MS(+) spectra of EuODO2A^{+} at pH 7.36. [EuODO2A]$^{+}$ (*m*/*z*: 438, 440; left), [Eu(ODO2A)(OH) + H]$^{+}$ (*m*/*z*: 456, 458; left), [Eu_2-$(ODO2A)_2(OH)_2$ + H]$^{+}$ (*m*/*z*: 911, 913, 915; right). Eu isotope abundance, Eu^{151} : Eu^{153} = 47.8% : 52.2%.

Density function theory calculations

The density function theory (DFT) calculated lowest energy structures of the EuDO2A$(H_2O)_3^{+}$ and EuODO2A$(H_2O)_3^{+}$ complexes are shown in Fig. 5. The DFT calculation method used was similar to those published and established for many complex systems including those of trivalent lanthanide complexes.[20] The selected bond lengths of the two complexes together with those of [Gd(ODO3A)$(H_2O)]^{+}$,[21] and [Gd-(DO3A)][22] are listed in Table 2 for comparison. Note that B3LYP calculations in combination with large-core ECPs are known to overestimate Ln–N distances. For example, the average crystal and our DFT calculated (in parentheses) Eu–N and Eu–O(carboxylate) bond distances for the EuDOTA^{-} complex are 2.68 Å (2.73 Å) and 2.38 Å (2.36 Å), respectively. An overestimation of the Eu–N bond distance by 0.05 Å and an underestimation of the Eu–O bond distance by 0.02 Å compared to crystal structural data have been observed in the present DFT study.

In the EuDO2A$(H_2O)_3^{+}$ structure, the 3 inner-sphere coordinated water molecules are arranged in a *meridional* configuration,[3c,23] *i.e.* the 3 water molecules are on the same plane perpendicular to that of the basal N_4 atoms. For the EuODO2A-$(H_2O)_3^{+}$ complex, the position of the middle coordinated water molecule is slightly moved away from the plane perpendicular to that of the basal N_3O atoms. However, the Eu(III)–O (apical H_2O) bond distance is longer than the other two Eu(III)–O (side H_2O) bond distances for each complex. Thus, dinuclear species formation could only result in the form of $Ln_2L_2(\mu\text{-}OH)_2$. The formation of tri-hydroxo-bridged dinuclear species is unlikely for the Ln(III)-DO2A^{2-} and Ln(III)-ODO2A^{2-} complex systems.

Owing to the slow convergence of the geometry optimizations for the dinuclear Eu(III)-ODO2A^{2-} systems in aqueous solution as experienced by us and others,[15f] a Y(III) ion was used as a substitute for the Eu(III) ion in these systems for DFT calculations. The ionic radii of Y(III) (1.019 Å) and Eu(III) (1.066 Å) ions are similar,[24] and they both belong to the rare-earth element family due to chemical similarities, although the Y(III) ion has no 4f electrons. Thus, the configurations of YDO2A^{+}, YODO2A^{+}, EuDO2A^{+} and EuODO2A^{+} are expected to be similar, except that the Eu(III) complexes are 9-coordinated with three inner-sphere coordinated H_2O molecules, the Y(III) complexes are 8-coordinated with two inner-sphere coordinated H_2O molecules. Attempts to either add or reduce inner-sphere coordinated H_2O molecules resulted in higher energies for both Eu(III) and Y(III) complexes. On the other hand, the lack of 4f electrons allows the DFT calculations of the Y(III) complexes to run faster than those for Ln(III) complexes.

The DFT calculated low-energy structures of the μ-OH bridged $Y_2(ODO2A)_2(\mu\text{-}OH)$ dinuclear species are shown in Fig. 6. Two structures are illustrated for the mono-μ-OH bridged dinuclear species: one with the lowest energy has one μ-OH bridge and a H_2O–Y–Y–OH_2 torsional angle of 82.21° (*cis*-$[Y_2(ODO2A)_2(\mu\text{-}OH)(H_2O)_2]^{+}$, −2326.666586 a.u.; Fig. 6, upper-left). The other with higher energy has one μ-OH bridge and a H_2O–Y–Y–OH_2 torsional angle of 148.54° (*trans*-

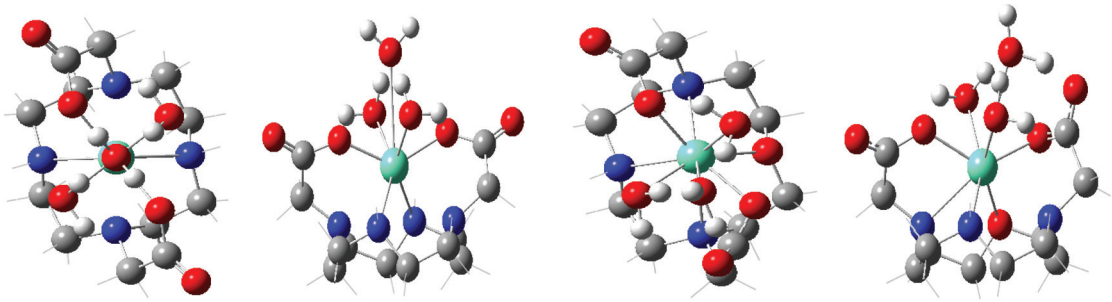

Fig. 5 DFT calculated $EuDO2A(H_2O)_3^+$ (left two structures, top- and side-views) and $EuODO2A(H_2O)_3^+$ (right two structures, top- and side-views) structures.

Table 2 DFT calculated selected bond lengths (Å) in $[EuDO2A(H_2O)_3]^+$ and $[EuODO2A(H_2O)_3]^+$, as compared with those of [GdODO3A(H_2O)] and $[GdDO3A]_3Na_2CO_3$ molecules[a,b,c]

	$[EuDO2A(H_2O)_3]^+$	$[EuODO2A(H_2O)_3]^+$	[GdODO3A]	$[GdDO3A]_3Na_2CO_3$
Eu–Oa (H_2O)	2.644	2.762	2.559	2.46[c]
Eu–O1 (H_2O/COO–)[a]	2.619	2.580	2.328	2.46[c]
Eu–O2 (COO–)	2.293	2.267	2.357	2.35
Eu–O3 (H_2O/COO–)[b]	2.619	2.539	2.351	2.34
Eu–O4 (COO–)	2.293	2.253	2.327	2.35
Eu–N5/O5	2.708	2.551	2.574	2.56
Eu–N6 (3°)	2.631	2.714	2.674	2.63
Eu–N7 (2°)	2.708	2.657	2.644	2.60
Eu–N8 (3°)	2.631	2.788	2.674	2.59
Eu–N_4/N_3O plane	1.650	1.70	1.633	1.55
Eu–COO^- plane			0.720	0.75

[a] For $DO2A^{2-}$ and $ODO2A^{2-}$, Oa is the apical H_2O molecule. O1 and O3 are the two side H_2O molecules. O2 and O4 are the oxygen atoms of the two COO^- groups. For $DO3A^{3-}$ (1,4,7,10-tetraazacyclododecane-1,4,7-triacetate ion) and $ODO3A^{3-}$ (also abbreviated as DOTRA, 1-oxa-4,7,10-triazacyclododecane-4,7,10-triacetate ion), O3 is the oxygen atom of the middle COO^- group. [b] [Gd(ODO3A)] data were obtained from crystal data, ref. 21. $ODO3A^{3-}$ is 7-coordinated, the complex has one apical coordinated water molecule (Oa), and the remaining coordination site is shared with a carboxylate group of a neighboring complex (O1). [c] Values are from reference crystallographic data, ref. 22. The bond distances are the two Eu–O bonds with the coordinated carbonate anions.

$[Y_2(ODO2A)_2(\mu\text{-}OH)(H_2O)_2]^+$, −2326.4103883 a.u.; Fig. 6, upper-right). A structure of a di-μ-OH bridged dinuclear species is also shown in Fig. 6 (lower-middle, $[Y_2(ODO2A)_2(\mu\text{-}OH)_2]$). It is observed that each Y(III) ion is 8-coordinated in the three complex structures shown in Fig. 6. The first and the second include 6-coordination by the ligand $ODO2A^{2-}$, one by the bridged μ-OH ion and one by a water molecule. The third includes 6-coordination by the ligand $ODO2A^{2-}$ and two by the bridged μ-OH ions.

The two inner-sphere coordinated water molecules in the $[Y_2(ODO2A)_2(\mu\text{-}OH)(H_2O)_2]^+$ dinuclear species are in a staggered conformation with a torsional angle of 82.21° or 148.54°. It is possible that the structure with one additional inner-sphere coordinated water molecule on each Y(III) ion at the available coordinating space of the $[Y(ODO2A)]_2(\mu\text{-}OH)_2$ dinuclear species is also present because both $\beta_{22\text{-}3}$ and $\beta_{22\text{-}4}$ values could be fitted from the Y(III)-$ODO2A^{2-}$ titration data. Selected average bond distances and angles of these four complexes are listed in Table S2 (ESI†).

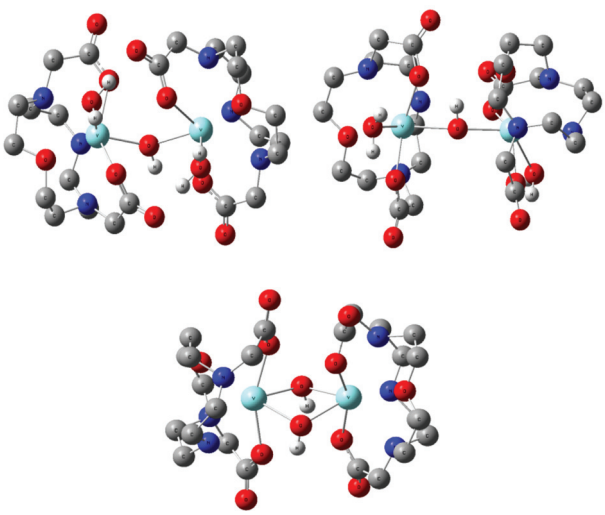

Fig. 6 DFT calculated structures of *cis*-$[Y_2(ODO2A)_2(\mu\text{-}OH)(H_2O)_2]^+$ (upper-left), *trans*-$[Y_2(ODO2A)_2(\mu\text{-}OH)(H_2O)_2]^+$ (upper-right), $[Y_2(ODO2A)_2(\mu\text{-}OH)_2]$ (lower-middle).

Luminescence studies

Fig. S4 (ESI†) show the emission spectra of the $EuODO2A^+$ complex at pH 6.1 in H_2O and D_2O, respectively, at room temperature (λ_{ex} = 395 nm). These spectra are very similar to those measured at pH 7.0 and pH 5.0. The lifetime data for the emission peak at 615 nm of the $EuODO2A^+$ complex in both

H_2O and D_2O solutions at pH 7.0 could be fitted to a single exponential luminescence decay kinetic equation. Similarly, the emission spectra (λ_{ex} = 369 nm, Fig. S5, ESI†) and the emission lifetime data at 544 nm of the $TbODO2A^+$ complex at pH 7.0 in H_2O and D_2O, respectively, have been obtained at room temperature. Table 3 lists the lifetime data and the numbers of inner-sphere coordinated water molecules (q) of the $EuODO2A(H_2O)_q^+$ and the $TbODO2A(H_2O)_q^+$ complexes obtained using the lifetime data by employing different previously established empirical equations.[25] For comparison purposes, those of the $EuDO2A(H_2O)_q^+$ complex are also included.[11]

The q values obtained for the $EuODO2A(H_2O)_q^+$ and $EuDO2A(H_2O)_q^+$ complexes from empirical equations $q^{a–d}$ were all greater than that from equation q^e. The early empirical equation q^a by Sudnick and Horrocks quoted an uncertainty value of ±0.5 for the q values obtained probably due to the lower number of experimental data used.[25a] This has been refined by equation q^e with a standard error of ±0.1 in q-values.[25e] For the derivation of the parameters for equation q^b by Beeby *et al.*,[25b] no species with q values greater than 6 were employed and the results for q values tend to be on the higher side. For equations q^c and q^d, it assumes that the quenching effects in D_2O are similar for all Eu^{3+} complexes and certainly provided only rough estimates of the q values.[25c,d] It is noted that these five equations all assumed that the contributions from the alcoholic O–H, amine N–H, alkane C–H and amide carbonyl oscillators in the first coordination sphere of the Eu^{3+} complex were negligible which is certainly not always true.[11,25f,g]

Ideally, lifetime measurements should be carried out without deuterium exchange of NH groups, so that these oscillators would contribute to the same extent to quench lanthanide luminescence. It has been found that deuterium exchange is very slow for NH groups coordinated to lanthanide ions.[26] To check the effect of the N–H oscillator, the lifetime of $EuODO2A^+$ in freshly prepared D_2O solution without drying and redissolving was measured and it was found that τ_{D2O} (1.42 ms) was the same as that with drying and redissolving. This indicates that H/D exchange in the $EuODO2A^+$ complex at pH 7.0 is probably slow within the D_2O solution preparation time period and the lifetime result obtained in D_2O solution is valid for the estimation of q value.

The averaged q value for the $EuODO2A(H_2O)_q^+$ complex is 4.1 which is greater than that of the $EuDO2A(H_2O)_q^+$ complex (q = 3.0), indicating that the complex has structures with an average of four inner-sphere coordinated water molecules. Thus, although the DFT calculated structure has the lowest energy with q = 3 (*vide supra*), it might still be possible that this complex could have equilibrium structures accommodating four or more inner-sphere coordinating water molecules. This might be due to the fact that the 12-membered macrocyclic ring of $ODO2A^{2-}$ is smaller, less symmetrical, not pre-organized[20e] and more rigid which may lead to more coordination space available for more inner-sphere coordinated water molecules on the Ln(III) ion. Similar results have been observed for other Eu(III) complexes of multidentate ligands with oxaaza backbones.[14,27,28] Note that the DFT calculated $EuODO2A^+$ structure showed that the Eu–O5 bond distance (2.55 Å) is shorter than the three Eu–N(6–8) bond distances (averaged 2.72 Å) leading to a less-symmetrical coordination environment as compared to that of the $EuDO2A^+$ complex. [Care should be exercised here to note that an overestimation of the Eu–N (*e.g.* 0.05 Å) bond distance and an underestimation of the Eu–O bond distance (*e.g.* 0.02 Å) are known in the present DFT study (*vide supra*).] This could allow other complex conformations with similar or slightly higher energies to occur and with one more coordinated water molecule. In addition, it is also possible that the oxygen atom and the secondary nitrogen atom in the macrocycle may have additional unusual effects in helping the complex to relax from the excited state.

For comparison purposes, the number of inner-sphere coordinated water molecules of $TbODO2A^+$ has also been measured[25a,b,d] to be 2.9 which is consistent with the expected q = 3 and previously reported values of several Tb(III) complexes of linear and macrocyclic multidentate ligands.[28] For example, the average q value in the pH range 4–11 is 1.8 ± 0.2 for TbDO3A ($DO3A^{3-}$ is 1,4,7,10-tetraazacyclododecane-1,4,7-triacetate ion) because $DO3A^{3-}$ is a 7-coordinating ligand and Tb(III) ion is 9-coordinated.[28b]

An interesting pH-dependence effect is observed for the luminescence emission spectra of the $EuODO2A^+$ complex, *i.e.* the spectral band intensity at 615 nm increases with increasing pH (Fig. 7). The lifetimes (in ms) are roughly constant from pH 5 to pH 7 and increase with increasing pH afterwards: 0.218 (pH 4.0), 0.220 (pH 5.0), 0.220 (pH 6.1), 0.219 (pH 7.0), 0.232 (pH 8.0), 0.257 (pH 9.0), 0.283 (pH 10.0), and 0.291 (pH 11.0). The gradual increase with increasing pH of lifetimes after pH 7.0 is consistent with the fact that the number of O–H oscillators decreases with increasing pH due to μ-OH bridged dinuclear species as well as mono-coordinated-OH formations. Similar observations have been found for the $TbODO2A^+$ complex (data not shown).

Conclusions

The log K_f values of the $LnODO2A^+$ complexes increase roughly with increasing lanthanide atomic number which

Table 3 The luminescence lifetimes (τ, ms) and the numbers of inner-sphere coordinated water molecules (q) of the $EuODO2A(H_2O)_q^+$ complex (λ_{ex} = 395 nm, λ_{em} = 615 nm, pH 7.0) and $TbODO2A(H_2O)_q^+$ complex (λ_{ex} = 369 nm, λ_{em} = 544 nm, pH 7.0)

Species	τ_{H2O}	τ_{D2O}	q^a					q_{ave}
$EuODO2A(H_2O)_q^+$	0.219	1.42	4.0[b]	4.3[c]	4.1[d]	4.3[e]	3.9[f]	4.1(.2)
$TbODO2A(H_2O)_q^+$	0.980	2.93	2.7[g]	2.9[h]	3.1[i]	—	—	2.9(.2)
$EuDO2A(H_2O)_q^+$[11]	0.280	1.34	3.0	3.1	3.1	3.2	2.8	3.0(.2)
$EuDO2A(OH)(H_2O)_q$[11]	0.313	1.46	2.6	2.7	2.7	2.8	2.4	2.6(.2)

[a] Empirical equations for $EuODO2A^+$: [b] $q^a = 1.05(\tau_{H2O}^{-1} - \tau_{D2O}^{-1})$; [c] $q^b = 1.2(\tau_{H2O}^{-1} - \tau_{D2O}^{-1} - 0.25)$; [d] $q^c = (1.05\tau_{H2O}^{-1} - 0.70)$; [e] $q^d = (1.1\tau_{H2O}^{-1} - 0.71)$; [f] $q^e = 1.1(\tau_{H2O}^{-1} - \tau_{D2O}^{-1} - 0.31)$. For $TbODO2A^+$: [g] $q^f = 5.0(\tau_{H2O}^{-1} - \tau_{D2O}^{-1} - B)$, $B = 0.06 + 0.09n^{NH}$, for ODO2A $B = 0.06 + 0.09 = 0.15$; [h] $q^g = 4.20(\tau_{H2O}^{-1} - \tau_{D2O}^{-1})$; [i] $q^h = (4.0\tau_{H2O}^{-1} - 1.0)$.

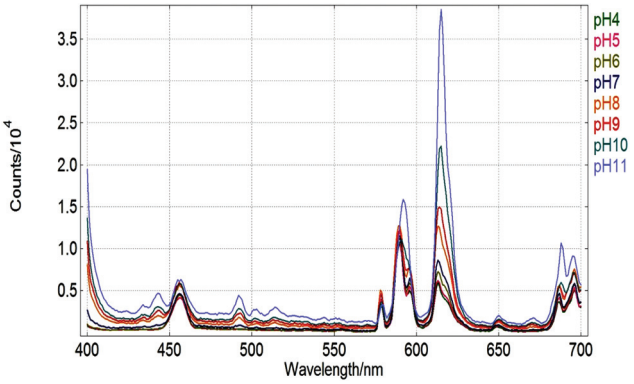

Fig. 7 Luminescence spectra of the $EuODO2A^+$ complex at various solution pH. λ_{ex} = 395 nm.

indicates that the bonding is mainly electrostatic in nature with some macrocycle size selectivity. The $LnODO2A^+$ complex formations are relatively faster as compared to those of the $LnDO2A^+$ complexes. This allows the determinations of formation constants of various hydrolytic species according to an unprecedented general hydrolysis scheme involving the stepwise and simultaneous formations of mono- and di-nuclear macrocyclic $LnODO2A^+$ complexes. The dinuclear structures are generally more abundant than the mononuclear ones. Mass spectrometry confirmed the presence of $[Eu(ODO2A)]^+$, $[Eu(ODO2A)(OH) + H]^+$, $[Eu_2(ODO2A)_2(OH_2)_2 + H]^+$, $[Eu(ODO2A)(OH)_2]^-$ and $[Eu_2(ODO2A)_2(OH_2)_3]^-$ species at pH higher than 7. The density function theory (DFT) calculated structures of the $EuODO2A(H_2O)_3^+$ and $EuDO2A(H_2O)_3^+$ complexes indicate that the 3 inner-sphere coordinated water molecules are arranged in a *meridional* configuration, *i.e.* the 3 water molecules are nearly on the same plane perpendicular to that of the basal N_3O or N_4 atoms. However, luminescence lifetime studies reveal that the $EuODO2A^+$ and $TbODO2A^+$ complexes has 4.1 and 2.9 inner-sphere coordinated water molecules, respectively, indicating that other equilibrium species are also present for the $EuODO2A^+$ complex. Additional DFT calculations show that each Y(III) ion is 8-coordinated in the three possible *cis*-$[Y_2(ODO2A)_2(\mu\text{-}OH)(H_2O)_2]^+$, *trans*-$[Y_2(ODO2A)_2(\mu\text{-}OH)(H_2O)_2]^+$ and $[Y_2(ODO2A)_2(\mu\text{-}OH)_2]$ dinuclear complex structures. The first and second include 6-coordination by the ligand ODO2A, one by the bridged μ-OH ion and one by a water molecule. The third includes 6-coordination by the ligand $ODO2A^{2-}$ and two by the bridged μ-OH ions. The two inner-sphere coordinated water molecules in the *cis*- and *trans*-$[Y(ODO2A)]_2(\mu\text{-}O(H_2O)_2]^+$ dinuclear species are in a staggered conformation with torsional angles of 82.21° and 148.54°, respectively. These results will be very useful for the design of ligands that form dinuclear Ln(III) complexes for various analytical and biomedical applications.

Experimental

Materials and standard solutions

Analytical reagent-grade chemicals and buffers, unless otherwise stated, were purchased from Sigma (St. Louis, MO, USA), Aldrich (Milwaukee, WI, USA) or Merck (Dammstadt, Germany) and were used as received without further purification. Disodium ethylenediaminetetraacetic acid (Na_2H_2EDTA) was purchased from Fisher. The ligand H_2ODO2A was prepared and purified as described below. Carbonate-free deionized water was used for all solution preparations.

The concentration of the H_2ODO2A stock solution (*ca.* 0.01 M) was determined by pH titration using a standard tetramethylammonium hydroxide solution (0.1 M), and was also checked by complexometric back-titration.[11] The concentrations of the lanthanide nitrate stock solutions were *ca.* 0.01 M and were standardized by EDTA titration using xylenol orange as the indicator. The EDTA solution was standardized by titrating a calcium carbonate primary standard solution (first dissolved in HCl solution) at pH 10 using calmagite as the indicator.

The 0.1 M tetramethylammonium hydroxide solution was prepared by diluting a 20% $(CH_3)_4NOH$–methanol solution obtained from Aldrich (carbonate-free). The aqueous $(CH_3)_4NOH$ solution was standardized by using reagent grade primary standard potassium hydrogen phthalate. A 0.1 M HCl solution was prepared by diluting a reagent grade HCl solution and standardized by using the standard $(CH_3)_4NOH$ solution. A 1.0 M stock solution of tetramethylammonium chloride (Aldrich) was prepared and diluted to 0.1 M for each titration to maintain a constant ionic strength (0.1 M).

Synthesis of H_2ODO2A

The compound was synthesized according to a published method with minor modification.[15] *N*,*N*,*N*-Tri(*p*-toluensulfonyl)-diethylenetriamine was first prepared and purified using the tritosylated diethylenetriamine (yield 75%, m.p. 176–177 °C) and was added equivalent amount of 1,5-bis(*p*-toluenesulfonyl)-3-oxapentane (yield 92%, m.p. 81–82 °C) to form the macrocycle 4,7,10-tris(*p*-tolysulphonyl)-1-oxa-4,7,10-triazacyclododecane (yield 77%, m.p. 196–198 °C). 1-Oxa-4,7,10-triazacyclododecane was then obtained by reacting 4,7,10-tris(*p*-tolysulphonyl)-1-oxa-4,7,10-triazacyclo-dodecane with sulfuric acid (yield 72%, m.p. 78–79 °C). 4,10-Dicarboxymethyl-1-oxa-4,7,10-triazacyclododecane (ODO2A) in the hydrochloride form was finally obtained by carboxymethylation of 1-oxa-4,7,10-triazacyclo-dodecane with bromoacetate and recrystallization in ethanolic HCl solution (yield 35%). Anal. Calc. for $H_2ODO2A\cdot 2.7HCl\cdot H_2O$ ($C_{12}H_{23}N_3O_5\cdot 2.7HCl\cdot H_2O$): C, 35.51; H, 6.88; N, 10.36. Found: C, 35.53; H, 6.89; N, 10.12. NMR (D_2O-DSS), ^{13}C: δ 42.05, δ 50.35, δ 52.59, δ 55.58, δ 66.29, δ 170.0 ppm; ^1H: δ 3.26, 3.27, 3.28, δ 3.34, 3.35, δ 3.68, 3.69, 3.70, δ 3.89 ppm. ESI(+)MS, *m*/*z* 290.1.

Potentiometric titrations

Acid–base and complex formation titrations were carried out at a constant ionic strength of 0.10 M $(CH_3)_4NCl$ using reported procedures.[11] A model 720 Metrohm Titroprocessor in conjunction with Metrohm Combination Electrode was employed to monitor the pH. Generally, equal molar concentrations of the ligand and the metal ion were employed (~1.0 mM) for the titration. The ionic strength of the solution was adjusted to 0.1 M using 1 M

$(CH_3)_4NCl$. The $(CH_3)_4NOH$ solution was delivered from a 10 mL automatic Brinkmann Metrohm Model 665 Dosimat buret with a reading accuracy of ±0.001 mL. Most of the titration reactions reached equilibrium rather quickly during the potentiometric titration process, and the titrations were completed within 18 000–40 000 s.

The pH-metric titration data were used to calculate the stepwise ligand protonation constants defined in eqn (1), where n = 1–4 for ODO2A (L):

$$K_n = [H_nL]/([H_{n-1}L][H^+]) \quad (1)$$

All equilibrium calculations were performed using the program Hyperquad2008 Version 5.2.15. The averaged values are presented together with the standard deviations calculated from valid data points. Speciation diagrams were generated using Hyss 2006 software.

Mass spectral measurements

Mass spectra of the Eu(III)-ODO2A^{2-} complex system at various pH were acquired by direct infusion (10 μL). ESI(+)MS experiments were carried out using a LTQ-Orbitrap hybrid tandem mass spectrometer (ThermoFisher, USA) equipped with an electrospray ionization (ESI) source operating in positive ion mode. The parameters of ESI(+) included 4.0 kV for ion spray voltage, 200 °C for capillary temperature, and 3–5 erb for sheath gas flow rate. The mass spectra were collected over the mass range of m/z 150–2000 at a resolving power of 30 000. The collected data were analyzed using Xcalibur software (ThermoFisher, USA). ESI(−)-MS measurements were performed using a micromass triple quadrupole mass spectrometer equipped with an ESI source operating in negative ion mode. The conditions used for the ESI(−) interface included 500 (L h^{-1}) for desolvation gas, 52 (L h^{-1}) for cone gas, 3.2 kV for capillary voltage, 30 V for cone voltage and 250 °C for desolvation temperature.

NMR determinations of protonation sites

Solutions of ligand (0.1 mM) for ^{1}H NMR titrations were prepared in D_2O solution, and pD was adjusted with DCl or carbonate-free NaOD. The apparent pD (pH) of the ligand solutions was determined with a microelectrode and the final pD value was obtained from the equation pD = pH + 0.40. All chemical shifts were referenced to the 3-(trimethylsilyl)propionic acid-d_4 sodium salt.

Luminescence measurements

Steady-state luminescence experiments were carried out on an Edinburgh Instruments FSP920 fluorescence system equipped with a 450 W xenon arc lamp as the illumination source. Emission light was collected into a TMS300 Czerny-Turner configuration double grating monochromator and detected by a Hamamatsu R928P photomultiplier tube in the visible wavelength range. Spectra were recorded by use of F900 Fluorescence spectrometer software. Luminescence lifetimes were recorded by use of a μF920H flashlamp (lamp frequency: 100 Hz) as the excitation source with the multiple-channel single photon counting mode (MCS). Data was fitted by a nonlinear least-squares iterative technique (Marquardt-Levenberg algorithm).

For the LnODO2A$^+$ systems (Ln = Eu or Tb), all solutions were prepared from stock solutions of $Ln(NO_3)_3$ (~0.01 M) and H_2ODO2A (~0.01 M). The molar ratio of the H_2ODO2A and Ln^{3+} was *ca.* 1.00 : 0.99 to make sure that the ligand was in slight excess. All solutions were allowed to equilibrate for at least 12 h to ensure complete formation reaction prior to luminescence measurements. The sample solutions in D_2O were prepared by first evaporating the aqueous solutions in appropriate flasks to dryness using a high vacuum system. To each flask, D_2O was added to dissolve the solids, the solution was equilibrated for at least 1 h, dried again, and finally dissolved in D_2O to a cuvette for luminescence measurements. Freshly prepared complex solutions in D_2O without drying and redissolving were also prepared for comparative measurements. The corresponding numbers of inner-sphere coordinated water molecules were calculated using the lifetime data in H_2O and D_2O with established empirical equations.[19] All data were checked at least twice carefully.

Density function theory (DFT) computations of lanthanide complex structures

All calculations were performed employing HF and hybrid DFT with the B3LYP exchange correlation functional and the Gaussian 09 package. Full geometry optimizations of the [Eu(DO2A)$(H_2O)_3]^+$, [Eu(ODO2A)$(H_2O)_3]^+$, *cis*-[Y_2(ODO2A)$_2$-(μ-OH)$_2(H_2O)_2]^+$, *trans*-[Y_2(ODO2A)$_2$(μ-OH)$_2(H_2O)_2]^+$ and [Y_2(ODO2A)$_2$(μ-OH)$_2$] systems were obtained in vacuum by using the 3-21G and 6-31G* basis sets for carbon, hydrogen, nitrogen, and oxygen. For these complexes, for example, the lowest energy crystallographic structure of EuDOTA$^-$ [square antiprismatic, SAP, Λ(δδδδ)] from Cambridge Structural Database (CSD) was used to construct the initial guessed structures of the EuDO2A$^+$ complex by removing two opposite carboxylate groups. The initial guessed structures were refined by a lower level HF/3-21G method and then refined by DFT calculations using the B3LYP/6-31G* method to find the lowest energy complex structures. The quasi-relativistic effective core potential (ECP) of Stuttgart RSC 1997 ECP and the related [5s4p3d]-GTO valence basis set were applied to europium and yttrium atoms. This ECP treats [Kr]4d^{10}4f^n as fixed core, while only the 5s5p6s5d6p shell is taken into account explicitly. The procedure involved initial HF/3-21G optimization of the molecular system and refinement by using B3LYP/6-31G* basis set, both in gas phase. The geometries of the complexes were then fully optimized by B3LYP/6-31G* and ECP in aqueous solutions by using a polarizable continuum model (PCM). Frequency calculations with zero-point corrections were also performed with the lowest-energy conformers of the LnL$^+$ (Ln = Eu, Y; L = DO2A^{2-}, ODO2A^{2-}) complexes.

Acknowledgements

The authors wish to thank the National Science Council and the Atomic Energy Council of the Republic of China (Taiwan) for financial support (grant numbers NSC-98-2113-M-010-001-

MY3, NSC 96-NU-7-009-003, and NSC-100-2811-M-010-003) of this work.

References

1 (*a*) P. Caravan, J. J. Ellison, T. J. McMurry and R. B. Lauffer, *Chem. Rev.*, 1999, **99**, 2293–2352; (*b*) C. A. Chang, *Eur. J. Solid State Inorg. Chem.*, 1991, **28**, 237–244; (*c*) C. A. Chang, L. Francesconi, M. F. Malley, K. Kumar, J. Z. Gougoutas, M. F. Tweedle, D. W. Lee and L. J. Wilson, *Inorg. Chem.*, 1993, **32**, 3501–3508; (*d*) C. A. Chang, P. Sieving, A. D. Watson, T. M. Dewey, T. B. Karpishin and K. N. Raymond, *J. Magn. Reson. Imaging*, 1992, **2**, 95–98; (*e*) C. A. Chang, *Invest. Radiol.*, 1993, **28**, S21–S27; (*f*) J. Varadarajan, S. Crofts, J. D. Fellmann, J. C. Carvalho, S. Kim, C. A. Chang and A. Watson, *Invest. Radiol.*, 1994, **29**, S18–S20; (*g*) T. Z. Lee, T. H. Cheng, M.-H. Ou, C. A. Chang, G. C. Liu and Y. M. Wang, *Magn. Reson. Chem.*, 2004, **42**, 329–336; (*h*) V. Jacques and J. F. Desreux, *Top. Curr. Chem.*, 2002, **221**, 123–164; (*i*) P. Hermann, J. Kotek, V. Kubicek and I. Lukes, *Dalton Trans.*, 2008, 3027–3047.

2 (*a*) J.-C. G. Bunzli, *Chem. Rev.*, 2010, **110**, 2729–2755; (*b*) C. P. Montgomery, B. S. Murray, E. J. New, R. PAL and D. Parker, *Acc. Chem. Res.*, 2009, **42**, 925–937; (*c*) C. M. G. Dos Santos, A. J. Harte, S. J. Quinn and T. Gunnlaugsson, *Coord. Chem. Rev.*, 2008, **252**, 2512; (*d*) L. E. Jennings and N. J. Long, *Chem. Commun.*, 2009, 3511–3524; (*e*) S. Mizukami, K. Tonai, M. Kaneko and K. Kikuchi, *J. Am. Chem. Soc.*, 2008, **130**, 14376–14377.

3 (*a*) P. D. Beer and P. A. Gale, *Angew. Chem., Int. Ed.*, 2001, **40**, 486; (*b*) T. L. Esplin, M. L. Cable, H. B. Gray and A. Ponce, *Inorg. Chem.*, 2010, **49**, 4643–4647; (*c*) M. L. Cable, J. P. Kirby, K. Sorasaenee, H. B. Gray and A. Ponce, *J. Am. Chem. Soc.*, 2007, **129**, 1474–1475; (*d*) R. Pal, D. Parker and L. C. Costello, *Org. Biomol. Chem.*, 2009, **7**, 1525–1528.

4 (*a*) J. R. Morrow, *Comments Inorg. Chem.*, 2008, **29**, 169; (*b*) A. K. Yatsimirsky, *Coord. Chem. Rev.*, 2005, **249**, 1997; (*c*) B. N. Trawick, A. T. Daniher and J. K. Bashkin, *Chem. Rev.*, 1998, **98**, 939; (*d*) N. H. Williams, B. Takasaki, M. Well and M. J. Chin, *Acc. Chem. Res.*, 1999, **32**, 485; (*e*) A. Roigk, R. Hettich and H. J. Schneider, *Inorg. Chem.*, 1998, **37**, 751; (*f*) P. Hurst, B. K. Takasaki and J. Chin, *J. Am. Chem. Soc.*, 1996, **118**, 9982; (*g*) M. Komiyama and T. Takarada, Acid-promoted peptide bond hydrolysis, in *Metal Ions in Biological Systems*, ed. A. Sigel and H. Sigel, Marcel Dekker, New York, 2003, vol. 40, ch. 10, p. 355; (*h*) H.-J. Schneider and A. K. Yatsimirski, Lanthanide-catalyzed hydrolysis of phosphate esters and nucleic acids, in *Metal Ions in Biological Systems*, ed. A. Sigel and H. Sigel, Marcel Dekker, New York, 2003, vol. 40, ch. 11, p. 369; (*i*) M. Komiyama, Sequence-selective scission of DNA and RNA by lanthanide ions and their complexes, in *Metal Ions in Biological Systems*, ed. A. Sigel and H. Sigel, Marcel Dekker, New York, 2003, vol. 40, ch. 12, p. 463.

5 C. F. Baes and R. E. Mesmer, *The Hydrolysis of Cations*, Wiley, New York, 1976, pp. 129–146.

6 Z. Zhang, *Chem. Commun.*, 2001, 2521–2529.

7 G. D. Klungness and R. H. Byrne, *Polyhedron*, 2000, **19**, 99–107.

8 (*a*) R. V. Southwood-Jones and A. E. Merbach, *Inorg. Chim. Acta*, 1978, **30**, 77–82; (*b*) C. A. Chang, Y.-P. Chen and C.-H. Hsiao, *Eur. J. Inorg. Chem.*, 2009, 1036–1042.

9 (*a*) K. New, C. M. Andolina and J. R. Morrow, *J. Am. Chem. Soc.*, 2008, **130**, 14861–14871; (*b*) F. Aguilar-Prez, P. Gmez-Tagle, E. Collado-Fregoso and A. K. Yatsimirsky, *Inorg. Chem.*, 2006, **45**, 9502–9517.

10 (*a*) C. A. Chang, B. H. Wu and B. Y. Kuan, *Inorg. Chem.*, 2005, **44**, 6646–6654; (*b*) C. A. Chang, B. H. Wu and C.-H. Hsiao, *Eur. J. Inorg. Chem.*, 2009, 1339–1346.

11 C. A. Chang, F.-K. Shieh, Y.-L. Liu, Y.-H. Chen, H.-Y. Chen and C.-Y. Chen, *J. Chem. Soc., Dalton Trans.*, 1998, 3243–3248.

12 (*a*) C. A. Chang and M. E. Rowland, *Inorg. Chem.*, 1983, **22**, 3866–3869; (*b*) C. A. Chang and V. C. Ochaya, *Inorg. Chem.*, 1986, **25**, 355–358; (*c*) C. A. Chang, P. H. L. Chang and S. Qin, *Inorg. Chem.*, 1988, **27**, 944–946; (*d*) C. A. Chang, V. O. Ochaya and V. C. Sekhar, *J. Chem. Soc., Chem. Commun.*, 1985, 1724–1725.

13 M. T. S. Amorim, J. R. Ascenso, R. Delgado and J. J. R. Fraústo da Silva, *J. Chem. Soc., Dalton Trans.*, 1990, 3449–3455.

14 R. C. Holtz, S. L. Klakamp, C. A. Chang and W. D. Horrocks Jr., *Inorg. Chem.*, 1990, **29**, 2651–2658.

15 (*a*) M. Purgel, Z. Baranyai, A. de Blas, T. Rodrıguez-Blas, I. Banyai, C. Platas-Iglesias and I. Toth, *Inorg. Chem.*, 2010, **49**, 4370–4382; (*b*) U. Cosentino, G. Moro, D. Pitea, A. Villa, P. Carlo Fantucci, A. Maiocchi and F. Uggeri, *J. Phys. Chem. A*, 1998, **102**, 4606–4614; (*c*) O. V. Yazyev, L. Helm, V. G. Malkin and O. L. Malkina, *J. Phys. Chem. A*, 2005, **109**, 10997–11005; (*d*) L. Smentek and B. A. Hess Jr., *Collect. Czech. Chem. Commun.*, 2008, **73**, 1437–1456; (*e*) J. Notni, K. Pohle, J. A. Peters, H. Görls and C. Platas-Iglesias, *Inorg. Chem.*, 2009, **48**, 3257–3267; (*f*) M. Mato-Iglesias, T. Rodrıguez-Blas, C. Platas-Iglesias, M. Starck, P. Kadjane, R. Ziessel and L. Charbonniere, *Inorg. Chem.*, 2009, **48**, 1507–1518.

16 (*a*) M. T. S. Amorim, S. Chaves, R. Delgado and J. Dasilva, *J. Chem. Soc., Dalton Trans.*, 1991, 3065–3072; (*b*) S. Chaves, A. Cerva and R. Delgado, *J. Chem. Soc., Dalton Trans.*, 1997, 4181–4189.

17 M. Kodama, T. Koike, A. B. Mahatma and E. Kimura, *Inorg. Chem.*, 1991, **30**, 1270–1273.

18 A. Roca-Sabio, M. Mato-Iglesias, D. Esteban-Gómez, E. Toth, A. de Blas, C. Platas-Iglesias and T. Rodrıguez-Blas, *J. Am. Chem. Soc.*, 2009, **131**, 3331–3341.

19 (*a*) C.-C. Lin, C.-L. Chen, K.-Y. Liu and C. A. Chang, *Dalton Trans.*, 2011, **40**, 6268–6277; (*b*) V. C. Sekhar and C. A. Chang, *Inorg. Chem.*, 1986, **25**, 2061–2065.

20 (*a*) L. J. Charbonnière, R. Schurhammer, S. Mameri, G. Wipff and R. F. Ziesse, *Inorg. Chem.*, 2005, **44**, 7151–7160; (*b*) U. Cosentino, A. Villa, D. Pitea, G. Moro, V. Barone and A. Maiocchi, *J. Am. Chem. Soc.*, 2002, **124**, 4901–4909; (*c*) D. J. Feller, *J. Comp. Chem.*, 1996, **17**, 1571–1586; (*d*) K. L. Schuchardt, B. T. Didier, T. Elsethagen, L. Sun, V. Gurumoorthi, J. Chase, J. Li and T. L. Windus, *J. Chem. Inf. Model.*, 2007, **47**, 1045–1052; (*e*) H. Y. Lee, C.-L. Chen and C. A. Chang, *Dalton Trans.*, submitted for publication.

21 M. R. Spirlet, J. Rebizant, X. Wang, T. Jin, D. Gilsoul, R. N. Muller and J. F. Desreux, *J. Chem. Soc., Dalton Trans.*, 1997, 497–500.

22 C. A. Chang, L. Francesconi, M. F. Malley, K. Kumar, J. Z. Gougoutas, M. F. Tweedle, D. W. Lee and L. J. Wilson, *Inorg. Chem.*, 1993, **32**, 3501–3508.

23 T. Le Borgne, P. Altmann, N. Andre, J.-C. G. Bunzli, G. Bernardinelli, P.-Y. Morgantini, J. Weber and C. Piguet, *J. Chem. Soc., Dalton Trans.*, 2004, 723.

24 R. D. Shannon, *Acta Crystallogr., Sect. A: Cryst. Phys., Diffr., Theor. Gen. Crystallogr.*, 1976, **32**, 751–767.

25 (*a*) W. DeW. Horrocks Jr. and D. R. Sudnick, *Acc. Chem. Res.*, 1981, **14**, 384–392; (*b*) A. Beeby, I. M. Clarksin and R. S. Dickins, *et al.*, *J. Chem. Soc., Perkin Trans. 2*, 1999, 493–503; (*c*) P. P. Barthelemy and G. R. Choppin, *Inorg. Chem.*, 1989, **28**, 3354–3357; (*d*) T. Kimura and Y. Kato, *J. Alloys Compd.*, 1995, **225**, 284–287; (*e*) R. M. Supkowski and W. DeW. Horrocks Jr., *Inorg. Chim. Acta*, 2002, **340**, 44–48; (*f*) D. Parker and J. A. G. Williams, *J. Chem. Soc., Dalton Trans.*, 1996, 3613; (*g*) R. S. Dickins, D. Parker, A. S. de Sousa and J. A. G. Williams, *Chem. Commun.*, 1996, 697.

26 A. Rodríguez-Rodríguez, D. Esteban-Gómez, A. de Blas, T. Rodríguez-Blas, M. Fekete, M. Botta, R. Tripier and C. Platas-Iglesias, *Inorg. Chem.*, 2012, **51**, 2509–2521.

27 Y. Wang and W. DeW. Horrocks Jr., *Inorg. Chim. Acta*, 1997, **263**, 309–314.

28 (*a*) C. A. Chang, H. G. Brittain, J. Telser and M. F. Tweedle, *Inorg. Chem.*, 1990, **29**, 4468–4473; (*b*) X. Zhang, C. A. Chang, H. G. Brittain, J. M. Garrison, J. Telser and M. F. Tweedle, *Inorg. Chem.*, 1992, **31**, 5597–5600.

